2004 AIMETA International Tribology Conference, September 14-17, 2004, Rome, Italy

NUMERICAL ANALYSIS OF SEALING CONDITIONS IN ELASTOMERIC RINGS

Marco SILVESTRI, Edzeario PRATI, Alessandro TASORA

Dipartimento di Ingegneria Industriale, Università degli studi di Parma
Parco Area delle Scienze, 43100 Parma, Italy
Phone +390521905700, Fax +390521905705, E-mail: silve@ied.unipr.it

ABSTRACT

This paper describes the latest developments in a research, carried on during several years, aimed at investigating sealing conditions in elastomeric ring.
Seal's lip displacement near the dynamic clearance is measured with a strain gauge transducer in actual working conditions. A detailed study of transducer characteristics and limits is included.
Numerical models of clearance forming has been developed taking in account the effect of temperature, defining the material constituting properties according to empiric WLF function. Both 2D and 3D models give results very similar and compatible with experimental measurements. The tridimensional model makes use of the experimental data for investigating the influence of tangential strain on clearance frequency.

NOMENCLATURE

τ:	relaxation time	p_d:	dynamic stress
Ψ:	phase displacement	p_s:	static stress
ω:	shaft speed	p_t:	total stress
R_a:	surface roughness	t:	time
T_g:	vitreous transition temperature	x_d:	dynamic strain
e_d:	dynamic eccentricity	x_s:	static strain
e_s:	static eccentricity	x_t:	total strain

INTRODUCTION

Radial lip seals for rotating shafts are widely used to retain oil and exclude contaminants, often shielding bearings or journal boxes for rotating shafts. They are cheap, compact and can be used also in presence of vibrations or little radial runout.
Many types of seals are available, differing in material and geometry in order to be suitable for several operating conditions. In spite of this variety, they are always built up by three fundamental elements: an elastomeric ring, a metallic stiffening insert and a garter spring (see Figure 1).

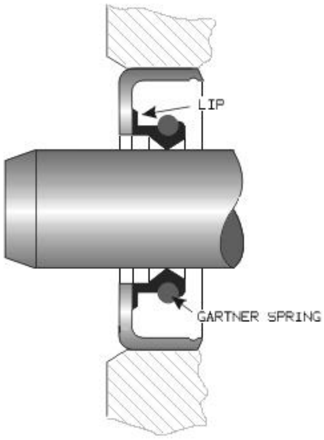

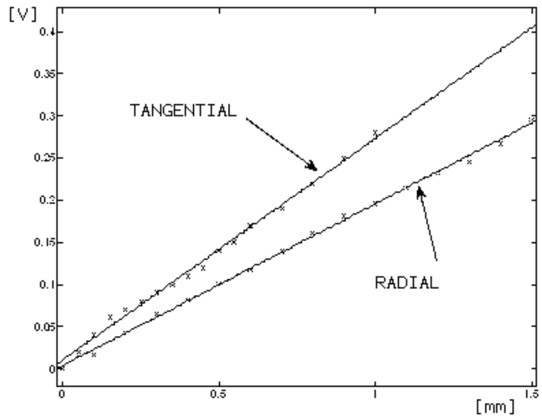

Figure 1. Outline of the seal assembly.

Figure 2. Transducer calibration curves.

The ring ends, at shaft interface, with a lip; the garter spring stiffens the lip and assures a better uniformity degree of the bearing pressure between seal and shaft on varying working conditions.

Investigations on the sealing and lubrication of radial lip seals have a long tradition [1], [2], [3], involving different disciplines as hydrodynamics, materials science and tribology. Their behaviour has been explained with the influence of temperature [4] and visco-elastohydrodinamic lubrication [5], [6], [7], but such explanations do not completely justify experimental results that show several stages of the leakage rate at different shaft rotating speed [8] [9] [10].

Preceding works have shown many experimental results achieved both in working conditions and with simulation apparatus by means of several transducers: cameras, torque meters, accelerometers (for *Frequency Response Function analysis*), thermocouples, flow measurements and, recently, a strain gauge transducer mounted on a machine that simulates actual operating conditions [10], [11].

Available experimental data also made possible to start implementing a numerical simulation of the phenomenon with Finite Elements Method. In [11] is described a first approach where dynamic seals behaviour was approximated by a non-linear Mooney-Rivlin model. This method was probed to be suitable for high frequencies rotating stress.

In order to reach a better synthesis of the tests results and the theoretical studies, we proceeded with experimental and numerical tests aimed at simulating temperature effects in actual working conditions.

TRANSDUCER ANALYSIS AND CALIBRATION

Previous works based on strain gauge transducer measurements [10], [11] emphasized the capacities of this method.

Now the construction has been optimized, calibration curves have been calculated and tangential signal is acquired contemporary with the radial one, allowing to know the phase displacement between them.

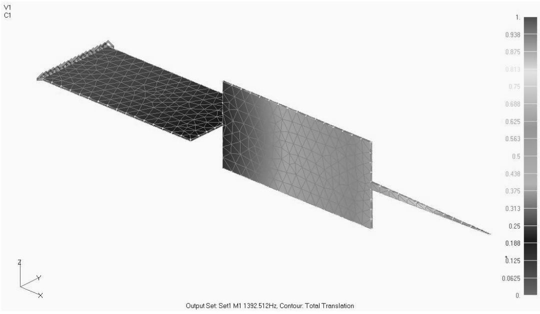

Figure 3. Transducer strain in working conditions.

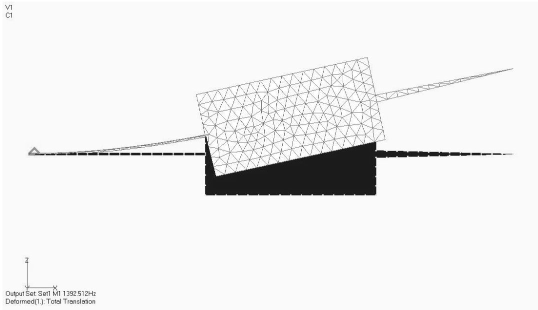

Figure 4. Transducer first natural frequency.

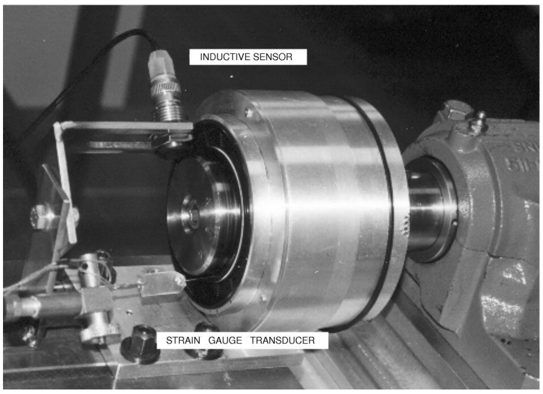

Figure 5. The test rig.

Thickness [mm]	Natural frequencies [Hz]		
	I	II	III
0,1	97	606	1697
0,15	145	909	2545
0,2	194	1213	3393
0,25	242	1519	4249

Table 1. Transducer natural frequencies

The transducer has been also validated by means of Finite Elements Method analysis software ABAQUS, using a model made of *tetrahedral* solid elements (see Figure 3). As a matter of fact, althought modelling a metallic foil could suggest using *plate* elements, solid elements allow a more realistic representation of the constraint between the cantilevers.
Figure 3 shows transducer strains in working conditions, while Figure 4 represent the first natural frequency of the system. As one can expects, it is the first flexural mode of a cantilever. Table 1 holds the values of first natural frequencies: with foil thickness of $0,25\ mm$ (the actual choosen thickness) frequencies are more than twice greater than $100\ Hz$, which corresponds to the maximum shaft speed during tests.
Calibration curves of both signals are shown in Figure 2. They have been calculated interpolating measurements obtained in 25 equally spaced points in the range of needle tip displacement of $0 \div 1,5\ mm$. Graphs highlight a good linearity in transducer response.

TEST RIG AND RESULTS

Test have been performed with the test rig used in [11]. Shortly, it is built up by a rotating shaft machine (see Figure 5) wih measuring and acquiring instruments.
The shaft is moved by a direct current electrical motor through a cogged belt transmission. Its speed may be continuosly regulated in the 300-6000 rpm range (at the output shaft).

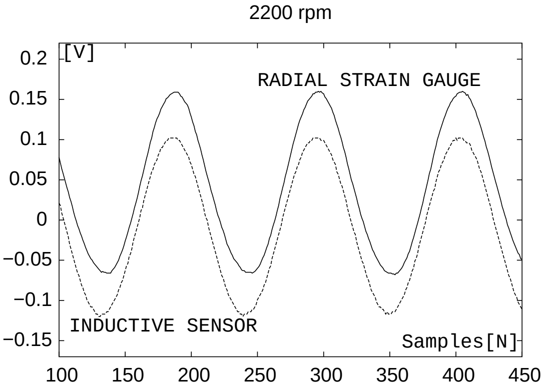

Figure 6. Lip and shaft profile radial displacements (sample rate 4000 Hz).

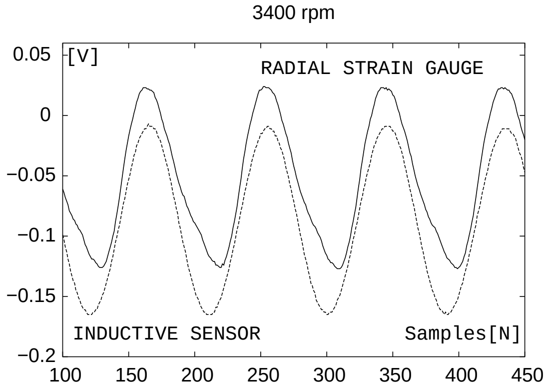

Figure 7. Lip and shaft profile radial displacements (sample rate 5000 Hz).

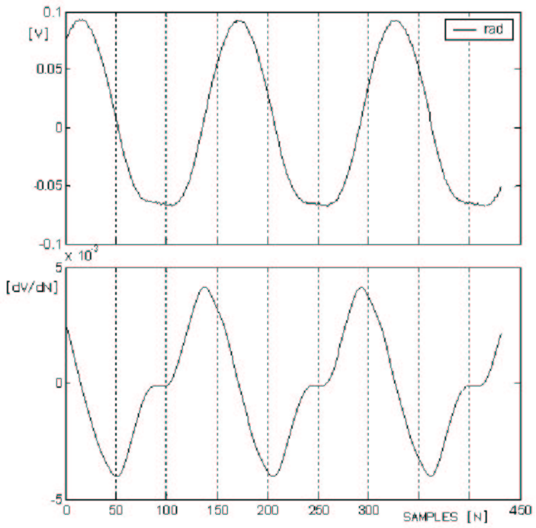

Figure 8. Radial signal and derivative of fitting function.

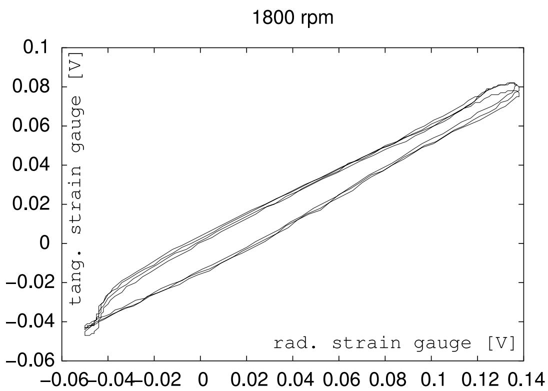

Figure 9. Hysteresis loop in case of clearance.

At the end, the shaft has a disk of circular profile which is in contact with the test seal. The dynamic eccentricity of this disk can be set to any value comprised between 0 and 0.52 mm by mean of a conical coupling. The disk is polished and has a surface roughness $R_a = 0.188\ \mu m$, as measured by using a profilometer. The position of the fixed seal housing can also be adjusted, giving the desired static eccentricity.

A fiber optics lamp lights the seal from the inside of the housing, allowing to directly verify, when the measures point out a clearance, the presence of a gap between the lip and the disk. The temperature of the sealing lip is monitored in three different points by using thermocouples.

It is known [8] [9] that working cycles have a great influence on the seal behaviour. In order to reach seal steady state, five working cycle of one hour at $1000\ rpm$ have been done.

Then, data have been collected varying the shaft speed between 500 and $6000\ rpm$ with steps of $100\ rpm$. Sampling rate vary from 1000 to $6000\ Hz$.

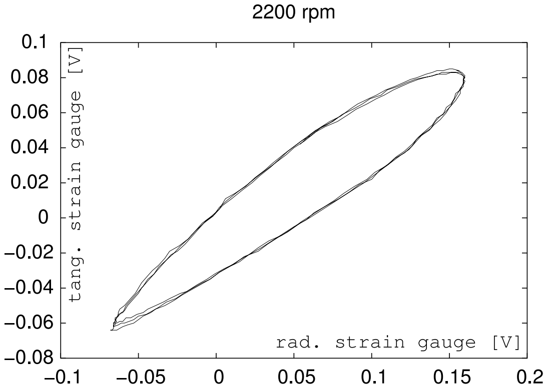

Figure 10. Hysteresis loop in case of sealing.

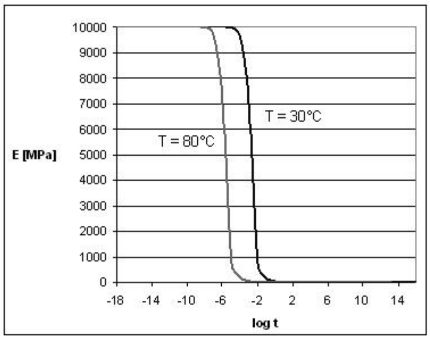

Figure 11. Relaxation curves shift due to temperature.

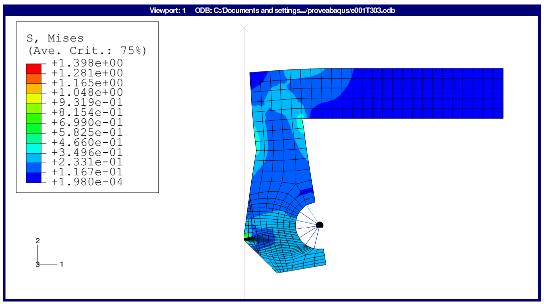

Figure 12. Von Mises stress in bidimensional model.

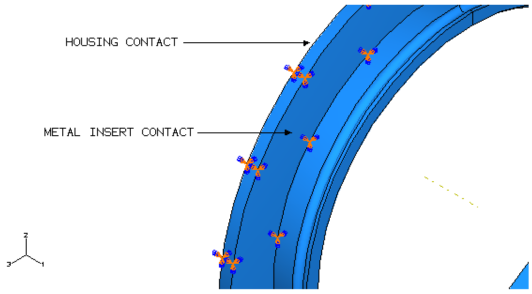

Figure 13. Tridimensional model of the seal.

Static and dynamic eccentricity are, respectively: $e_s = 0,2\ mm$, $e_d = 0,35\ mm$.
Results reflect the alternation of contact and clearance phases already observed in [8] and [11].
Figures 6 and 7 exemplifying the sealing running (here at $2200\ rpm$) and the next detaching.

NUMERICAL INTERPRETATION OF RESULTS

Graphs shown in Figures 6 and 7 qualitatively agree with theory [10]. A further effort has been spent in introducing an automated criterion for recognizing the presence of clearance, avoiding the subjective, not always unambiguous, interpretation of curves ”deviating” between each other.
To this end, two applications have been developed: first, in LabView environment, the acquiring tool has been enriched with an user friendly interface, allowing to adjust a low-pass filter that significantly improves redeability of signals, removing some transient noise that may be confused with clearance forming.
Moreover, a Matlab application for off-line signal computing has been used to evaluate some hypotesis of numerical definition of the phenomenon. Among them, the most useful seems to be studying the derivative of a function obtained as Fourier series approximation of acquired signal.

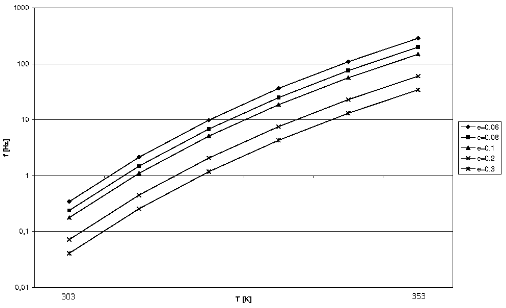

Figure 14. Clearance frequencies at different temperature and eccentricity (2D model).

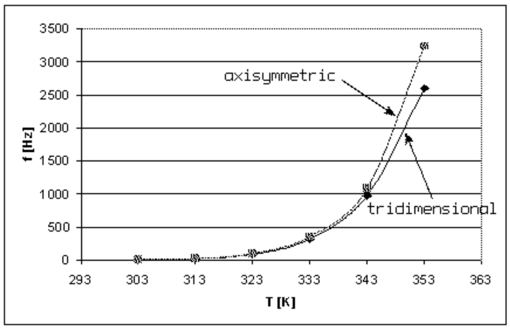

Figure 15. Comparison of clearance frequencies in 2D and 3D models.

It is necessary to pass through such a fitting function since derivating directly the signal results too much sensitive to measurements error, as often happens performing numerical derivative of tabular functions [12].
Graphs in Figure 8 clarify that this computation transforms the anomaly in the bottom part of the sine function in a univocaly, automatically indentifiable, piece of graph with zero slope.
Figures 9 and 10 show the hysteresis loop of the lip motion caused by the phase displacement between radial and tangential displacement. In particular, in case of lip detachment, a part of the hysteresis ellipse degenerates into a straight line and the overall loop area decreases.

FEM ANALYSIS

In [10] and [11] has been described a FEM seal model obtained as solid of rotation obtained from a simplified section and its reliability has been validated by means of a comparisons of experimental results of Frequency Response Function analysis.
This paper illustrates the enhancement of the model, that now takes in account temperature effects on material consitutive law, by means of repeating the simulation at varying elastomer temperature, so *Prony series*, that describes material constituting properties, changes according to empiric *Williams - Landell - Ferry* shift function. In other words, *WLF* relation gives the vitreous transition frequency shift at varying temperature conditions: increasing stress frequency up to transition zone the seal lip cannot follow shaft movement and clearance happens.
In detail, is possible to exploit ABAQUS ability to simulate varying boundary conditions applying to the seal lip a static strain x_s and a sinusoidal one $x_d(t)$, obtaining altogether:

$$x_t(t) = x_s + x_d(t) = x_s + |x_d| \cos \omega t \tag{1}$$

Correspondly, the total stress results:

$$p_t(t, y) = p_s(y) + p_d(t, y) = p_s(y) + |p_d(y)| \cos(\omega t + \Psi) \tag{2}$$

So is possible to suppose that the detachment happens if, in i^{th} node, where the stress is maximum, dynamic stress become greater than the static one, giving $p_t(t, y_i) < 0$. Physically

Prony series coefficients	
$g_1 = 0,9504$	$\tau_1 = 0,003[s]$
$g_2 = 0,045$	$\tau_2 = 0,072[s]$
$g_3 = 0,003$	$\tau_3 = 1,01[s]$
$g_4 = 0,0003$	$\tau_4 = 19,9[s]$
$g_5 = 0,00013$	$\tau_5 = 367[s]$
$g_6 = 0,00011975$	$\tau_6 = 3606[s]$
$g_7 = 0,0000828$	$\tau_7 = 47347[s]$

Table 2. *Prony* series coefficients

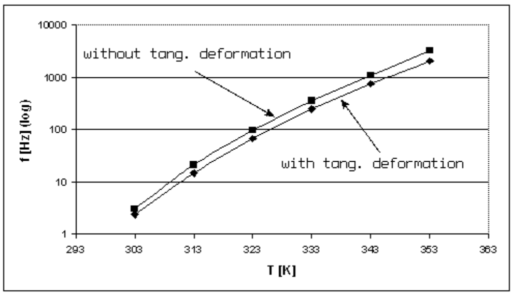

Figure 16. Effect of tangential stress (3D model).

this happen near to the vitreous transition of the elastomer, that cause a dramatic increasing in rubber stiffness.

Table 2 shows the *Prony* series coefficients used at reference temperature of $303\ K$, while the vitreous transition temperature has been estimated as $T_g = 253\ K$. Curves in Figure 11 exemplify as a relaxation curves shifts passing from reference temperature to working temperature ($353\ K$).

The geometric modeling has been make up both with a simplified 2D model (see Figure 13) and with a 3D model (see Figure 12). The first has been useful to quickly adjusting conditions and to verify results comparing with [5], while the 3D model, more realistic, takes in account also the tangential stress that the shaft generates on the contact surface.

Bidimensional and tridimensional models agree on clearance frequencies, as curves in Figure 15 show. Figure 16 highlights the contribution of tangential stress to reaching the clearance forming.

CONCLUSIONS

Measurements with a strain gauge transducer aimed to study clearance forming during rotating seals working have been improved and furnished with a deep analysis of sensor characteristics and limits.

A promising method of automated recognition of clearance forming has been found out: further development will include using this technique in real time.

Tangential strain measurements have allowed a better definition of the tridimensional FEM model of the seal, highlighting that its effect is not negligible.

Numerical 2D and 3D models give close results in terms of temperature - clearance frequency curves. These diagrams will be experimentally validated with a new test rig, now under construction, that will allow active control of lubricant temperature.

ACKNOWLEDGMENTS

This research was supported by the grant of the Università degli Studi di Parma.

The authors acknowledge the useful help of Ing. Alberto Mazzoni and Ing. Mattia Cenci in the experimental tests.

REFERENCES

[1] **Jagger E. T.,** *Study of the Lubrication of Synthetic Rubber Rotary Shaft Seals*, Proceedings of the Conference on Lubrication and Wear, I.Mech.E., pp. 409-415, 1957.

[2] **Müller, H.K.,** *Concepts of sealing Mechanism of Rubber Lip Type Rotary Shaft Seals*, Proceedings of the 11^{th} International Conference on Fluid Sealing, B.H.R.A., Paper K1, pp. 698-709, 1987.

[3] **Salant, R.F.,** *Numerical Analysis of the Flow Field Within Lip Seals Containing Microundulations*, ASME Journal of Tribology, Vol. 114, pp. 485-492, 1992.

[4] **Stakenborg, M.J.L.,** *On the Sealing Mechanism of Radial Lip Seals*, Tribology International, Vol. 21, pp. 335-340, 1988.

[5] **Stakenborg, M.J.L., van Leeuwen, H.J. and ten Hagen E.A.M.,** *Visco-Elastohydrodynamic (VEHD) Lubrication in Radial Lip Seals: Part I - Steady-State Dynamic Viscoelastic Seal Behavior*, ASME Journal of Tribology, Vol. 112, pp. 578-583, 1990.

[6] **van Leeuwen, H.J., and Stakenborg M.J.L.,** *Visco-Elastohydrodynamic (VEHD) Lubrication in Radial Lip Seals: Part 2 - Fluid Film Formation*, ASME Journal of Tribology, Vol. 112, pp. 584-592, 1990.

[7] **G. Colombo ed E. Prati,** *Condizioni di Tenuta con Guarnizioni Radiali per Alberi Rotanti*, atti del XV Congresso AIMETA di Meccanica Teorica e Applicata, 26-28 Settembre, Taormina, 2001. Sommario pag. SP ME 20.

[8] **M. Amabili, G. Colombo and E. Prati,** *Leakage of Radial Lip Seals at Large Dynamic Eccentricities*, Proceedings of the 16^{th} International Conference on Fluid Sealing, 18-20 September 2000, Brugge, Belgium, pp. 321-333.

[9] **M. Amabili, G. Colombo and E. Prati,** *On the Leakage of Radial Lip Seals*, Proceedings of 2000 AIMETA International Tribology Conference, 20-22 September, L'Aquila, Italy, pp. 565-572

[10] **M. Silvestri, E. Prati, A. Tasora,** *Un modello del comportamento di tenute dinamiche al variare della temperatura*, atti del XVI Congresso AIMETA di Meccanica Teorica e Applicata, 9-12 settembre, Ferrara 2003.

[11] **M. Silvestri, E. Prati, A. Tasora,** *Dynamic Seals Behaviour under Effect of Radial Vibration*, proceedings of 14^{th} International Colloquium Tribology, Tribology Lubrication Engineering, January 13-15, Stuttgart 2004.

[12] **F. B. Hildebrand,** *Introduction to Numerical Analysis*, Mc GRAW HILL, New York 1967